BMC Pharmacology and Toxicology

RESEARCH Open Access

Population pharmacokinetic analysis of febuxostat with high focus on absorption kinetics and food effect

Wenjun Chen[1], Bo Jiang[1], Zourong Ruan[1], Dandan Yang[1], Yin Hu[1] and Honggang Lou[1*]

Abstract

Febuxostat is commonly used in clinic for the treatment of hyperuricemia. Multiple-peak phenomenon has been observed in human plasma concentration-time profiles of febuxostat, but has not been paid enough attention in previous research. This study takes a pivotal step forward by conducting a comprehensive population pharmacokinetic (PopPK) analysis of febuxostat in a healthy Chinese cohort, with a central focus on delineating its absorption profile under contrasting fasting and fed conditions, while concurrently assessing the influence of food alongside other potential covariates on febuxostat's PK profile. The plasma concentration data used for modeling was obtained from two bioequivalence (BE) studies. Subjects were administered febuxostat 20 mg or 80 mg under fasting or fed condition. Goodness-of-fit plots, visual predict check (VPC), and normalized prediction distribution error (NPDE) were used for model evaluation. Based on the established model, PK profiles in healthy Caucasian subjects were simulated with parameter adjustment for race difference on clearance and bioavailability. Data from 128 subjects were used in the PopPK analysis. Febuxostat concentration-time curves were described by a two-compartment model with two deposit absorption compartments and lag times (Tlag). Prandial states (Food) showed significant impact on absorption rate ka1 and ka2, as well as Tlag1, and body weight was identified as a significant covariate on the apparent distribution volume. The PopPK analysis of febuxostat in healthy Chinese volunteers, under both fasted and fed conditions, successfully characterized its PK profile and underscored the significant influence of food on absorption. The potential difference of absorption between Chinese population and Caucasian population indicated from the simulations needs further investigation.

Keywords Population pharmacokinetics, Absorption, Kinetics, Food effect, Febuxostat

*Correspondence:
Honggang Lou
louhg@zju.edu.cn
[1]Center of Clinical Pharmacology, The Second Affiliated Hospital of Zhejiang University School of Medicine, Hangzhou, China

Introduction

Febuxostat (2-[3-cyano-4- (2-methylpropoxy)phenyl]-4-methylthiazole-5-carboxylic acid), approved for the treatment of hyperuricemia in adults with gout [1], is a nonpurine selective inhibitor of xanthine oxidase (XO) acting by decreasing the production of uric acid. Febuxostat is a weak acid, practically insoluble in water and slightly soluble in methanol. In the Biopharmaceutics Classification System (BCS), febuxostat is classified as a low-solubility high-permeability drug (BCS II) [2]. It has been reported that febuxostat is relatively rapidly absorbed after oral administration and reaches maximum plasma concentrations (C_{max}) after 0.5 ~ 1.5 h under fasting condition in humans [3]. Febuxostat undergoes both phase I and phase II metabolism. And it is extensively metabolized by glucuronidation (up to 40%) [3], mainly via uridine diphosphate-glucuronosyltransferase (UGT) UGT1A1, UGT1A3, UGT1A9, and UGT2B7 [4].

The majority of the pharmacokinetic (PK) studies have estimated the PK parameters of febuxostat employing conventional non-compartmental methodologies [3, 5–10], while a limited number of population pharmacokinetic (PopPK) analyses are documented in the existing literature [11–15]. Diverging from non-compartmental analysis (NCA), model-oriented approaches facilitate a superior approximation of drug kinetics and permit a deeper understanding of the pharmacokinetic process, encompassing aspects such as absorption, distribution and metabolism [16]. Studies in humans [3, 9, 17] have reported the observation of multiple peaks in the plasma concentration-time profiles of febuxostat, suggesting that the absorption of febuxostat may not follow a simple first-order pattern. However, in the published PopPK studies, the multiple-peak phenomenon and absorption kinetics of febuxostat has not been adequately addressed. A singular exception is the work by Rekić et al. [13], which proposed a two-compartment model featuring sequential zero-to-first-order absorption with a lag time, eschewing the simplicity of a linear first-order absorption model. Their investigation entailed a pooled PopPK analysis across a racially diverse cohort including healthy volunteers and patients diagnosed with gout or hyperuricemia; however, the fasting or fed status during febuxostat administration remains unspecified. It is a well-established fact that food intake can modulate the bioavailability of orally administered drugs by influencing drug solubility and gastric emptying rates, thereby potentially altering drug retention within the stomach [18]. Consequently, elucidating the impact of food on febuxostat's absorption kinetics is of paramount importance.

This study primarily aims to conduct a PopPK analysis of febuxostat in healthy Chinese subjects, with a particular emphasis on characterizing absorption under both fasting and fed conditions, while concurrently assessing the influence of food alongside other potential covariates on febuxostat's PK profile. Additionally, a supplementary objective entails utilizing the developed model to simulate PK profiles for different populations, probing for any disparities in febuxostat absorption characteristics or variations in the food effect on absorption between Asian and Caucasian populations.

Materials and methods

Study design and data source

Plasma concentration data employed in the PopPK analysis were obtained from two open-label bioequivalence (BE) studies, in healthy Chinese adult volunteers under both fasting and fed condition. The studies were conducted at the Center of Clinical Pharmacology, the Second Affiliated Hospital of Zhejiang University School of Medicine (Hangzhou, Zhejiang, China), in accordance with Good Clinical Practices and the ethical principles of the Declaration of Helsinki [19]. The study protocols were approved by the Human Research Ethics Committee of the study site. All participants gave written and informed consent before participating in any study-related procedures. Only concentration-time profiles after taking the reference drug were used in the PopPK modeling.

Details of the study design are elaborated upon in supplementary materials. Briefly, subjects received a single 20 mg or 80 mg dose of febuxostat in separate BE studies, with tablet administration accompanied by 240 mL of water. Participants fasted for a minimum of 10 h pre-dose in the fasting study, whereas a standardized high-fat and high calorie meal (800–1000 kcal) was consumed within 30 min of dosing in the fed condition. Sampling schedules varied slightly between doses but comprehensively covered the time course, with blood collections starting 30 min before dosing up to 48 h post-administration, depending on the study arm. Plasma was isolated via centrifugation at 3000 rpm and stored at −70 °C until analysis using a liquid chromatography-tandem mass spectrometry analysis method reported by Xu et al. [20]

Population pharmacokinetic analysis

Data obtained from the two BE studies were pooled for PopPK analysis. One-, two- and three-compartment models with first-order elimination were explored as structural model. In addition, several absorption models were investigated, including Weibull, variable exponential absorption, variable binomial absorption, zero and first-order simultaneous absorption, sequential zero to first-order with or without lag-time, and double gamma absorption model reported by Koloskoff et al. [21]. Log-normal distributions were assumed for all model parameters, with inter-individual variability (IIV) modeled exponentially. Residual variability was assessed using

proportional, additional, and combined proportional and additional error models.

The stepwise covariates modeling (SCM) method was employed for covariate selection, with criteria of $p<0.05$ for forward inclusion and $p<0.01$ for backward elimination. Demographic characteristics, including sex, age, body weight (WT) and body mass index (BMI) were evaluated for their influence on apparent clearance (CL/F) and distribution volume. Food intake was evaluated as a categorical covariate on the parameters relating to absorption (Eq. 1). Linear functions were used for continuous covariates as Eq. (2).

$$\log P = \log P_{TV} + \theta_{COV} \cdot Food \tag{1}$$

$$\log P = \log P_{TV} + \theta_{COV} \cdot \log\left(\frac{COV_i}{COV_m}\right) \tag{2}$$

Where P_{TV} represented the population parameter, while P was the individual parameter; θ_{COV} was the coefficient for the effect of the covariate, and COV_m was the median value of the covariates (COV_i). Food is 0 for the fasted state, and food equals 1 for the fed state.

The PopPK analysis was performed using the stochastic approximation estimation method (SAEM) via Monolix Suite® (version 2023R1, Lixoft SAS, a Simulations Plus company). Dataset preparation, exploratory analysis, and visualization were accomplished using R software (version 3.5.1, The R Foundation for Statistical Computing, http://www.r-project.org/). Model selection was based on Akaike Information Criteria (AIC), objective function value (OFV), goodness-of-fit (GOF) plots as well as the plausibility and stability of the model.

Model validation and simulations

Model validations were performed by visual predictive check (VPC) with 1000 simulations based on the parameter estimates of the established model. The results of VPC were exhibited by overlaying observed data with the median, and 5 and 95 percentile curves of the predictions with 1000 simulated replicates. Besides, normalized prediction distribution error (NPDE) was performed for model evaluation. The NPDE results were summarized graphically using a histogram of the NPDE, and scatterplots of NPDE versus time or population predictions.

Based on the final model, the plasma concentration-time curves of febuxostat under different administration schemes in Chinese population were simulated using a Monte Carlo method. Besides, the impact of significant covariates on the PK behavior of febuxostat were simulated at different levels of the covariate.

Simulation of PK profiles of febuxostat in Caucasian population was performed by adding the impact of race on PK parameters. Model parameters in the simulation were adjusted according to the covariate results reported by Rekić et al. [13] Specifically, CL/F was increased and relative bioavailability was decreased. Subsequently, the model simulated results were compared with the PK curves and parameters reported in the literature. The literature search process and details were described in the Supplementary material.

Non-compartmental and statistical analysis

Non-compartmentat analyses (NCA) were performed to obtain the key PK parameters of febuxostat in different scenarios, as well as to compare the observed and predicted PK characteristics. Generally, C_{max}, t_{max}, AUC_{0-t} and $AUC_{0-\infty}$were calculated and summarized. Student's *t* test was used to determine the significance between the fasted group and the fed group for C_{max}, AUC_{0-t}, and $AUC_{0-\infty}$. T_{max} was analyzed by Wilcoxon test. Difference at a level of $p<0.05$ was considered to be statistically significant.

Results

Dataset

A total of 2455 data points from 128 volunteers (including 81 male subjects and 47 female subjects) were used in the PopPK modeling. Concentration data below the lower limit of quantification were omitted for PopPK analysis. Demographic characteristics of the included population are presented in Table 1. The demographic characteristics of fasting population and fed population showed no obvious difference in both two studies. The mean plasma concentration-time profiles of febuxostat with standard deviation (SD) in the two BE studies grouped by prandial states were shown in Fig. 1. The main non-compartment

Table 1 Summary of the characteristics of the included subjects

	20 mg		80 mg	
	Fasting study	Fed study	Fasting study	Fed study
n	36	31	31	30
Male subjects, n (%)	23 (63.9%)	16 (51.6%)	21 (67.7%)	21 (70.0%)
Age (years), median [range]	27.5 [18.0–44.0]	29.0 [21.0–44.0]	26.0 [21.0–43.0]	26.5 [21.0–42.0]
Body weight (kg), median [range]	61.7 [45.4–73.6]	63.4 [46.3–79.0]	59.5 [47.1–73.7]	60.4 [49.0–78.4]
BMI (kg/m2), median [range]	21.7 [19.6–25.6]	22.8 [19.4–25.8]	21.3 [19.1–25.5]	22.4 [19.4–25.8]

BMI body mass index

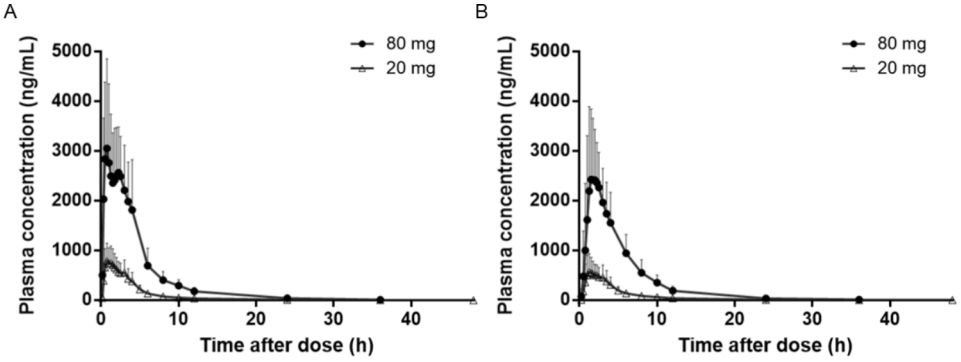

Fig. 1 Plasma concentration-time profiles of febuxostat grouped by dose and prandial states. Data were shown as mean and SD. (**A**) single administration of 20 mg or 80 mg febuxostat in the fasted state; (**B**) single administration of 20 mg or 80 mg febuxostat in the fed state

Table 2 Non-compartment pharmacokinetic parameters of febuxostat in the two BE studies

Parameter		T_{max} (h) (median, range)	C_{max} (ng/ml) (mean ± SD)	AUC_{0-t} (h*ng/ml) (mean ± SD)	$AUC_{0-\infty}$ (h*ng/ml) (mean ± SD)
20 mg	Fasting (36)	1.25 (0.33, 4.00)	1091 ± 301.0	3499.48 ± 756.66	3552.00 ± 752.93
	Fed (31)	1.50 (0.50, 3.50)	856.0 ± 253.7	2926.99 ± 751.55	2984.70 ± 761.04
	p value	0.28	0.00095	0.0021	0.0024
80 mg	Fasting (31)	1.00 (4.00, 0.33)	4327 ± 1254	15437.21 ± 3222.98	15549.11 ± 3229.06
	Fed (30)	1.75 (0.75, 4.00)	3432 ± 1148	13972.88 ± 4003.70	14086.00 ± 4007.47
	p value	0.095	0.0051	0.14	0.14

C_{max} maximum observed concentration, T_{max} time to reach the observed C_{max}, AUC_{0-t} area under the plasma concentration-time curve from time zero to the time for the last measurable concentration, $AUC_{0-\infty}$ area under the plasma concentration-time curve from time zero to infinity, SD standard deviation

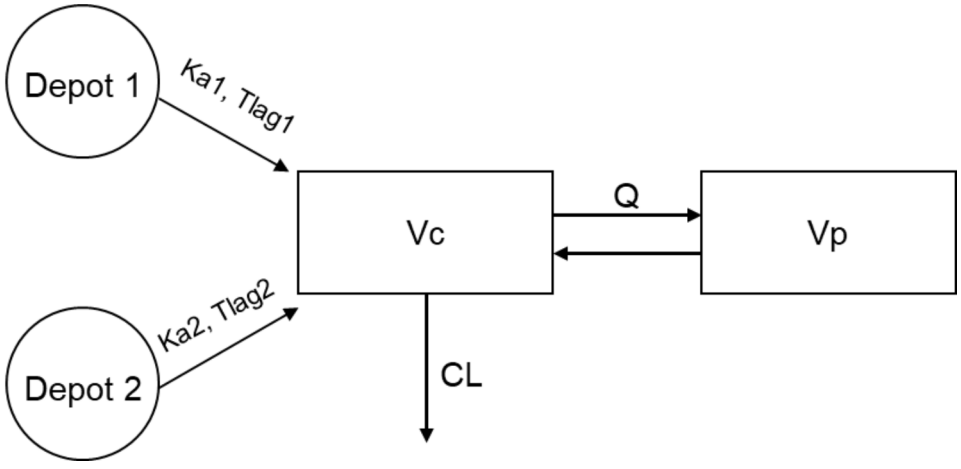

Fig. 2 Structural components of the population pharmacokinetic model

PK parameters of febuxostat in the two BE studies were summarized in Table 2. From the results of NCA in our study, C_{max} had significant difference between the fasted and fed population in both 20 mg and 80 mg group, while AUC did not show significant difference between fasted and fed groups in 80 mg group.

PopPK analysis

Plasma concentrations of febuxostat were well described by a two-compartment disposition model. The absorption of febuxostat was divided into two deposit compartments. The absorption from the first depot following a first-order kinetics with a rate constant ka1, and with a lag time Tlag1, accounted for F1 fraction of the absorbed febuxostat; the remainder absorption (1-F1) from the second depot started after a lag time Tlag2, followed a first-order kinetics with a rate constant ka2. Structural components of the PK model are shown in Fig. 2. After the SCM modeling process, prandial states (Food) showed significant impact on ka1, ka2 and Tlag1, and body weight was identified as a significant covariate on the apparent distribution volume of central

Table 3 Population pharmacokinetic parameters for the final model of febuxostat

Parameters	Final model estimates (RSE%)	IIV (CV%) (RSE%)	Shrinkage of conditional distribution (%)
ka1 (h^{-1})	4.02 (11.4)	101.11 (7.62)	−1.16
ka2 (h^{-1})	4.34 (15.6)	150.98 (7.72)	−13.6
F1	0.51 (3.7)	32.87 (7.24)	−0.499
Tlag1 (h)	0.22 (8.93)	81.13 (6.91)	−2.87
Tlag2 (h)	0.92 (7.63)	103.05 (6.64)	9.58
CL/F ($L{\cdot}h^{-1}$)	6.14 (2.26)	25.71 (6.44)	−0.725
V_c/F (L)	10.38 (2.07)	17.84 (10.6)	−9.03
Q/F ($L{\cdot}h^{-1}$)	1.93 (4.25)	37.81 (11.1)	8.66
V_p/F (L)	10.22 (3.21)	24.62 (10.9)	−11.5
Food_ka1	−2.04 (8)		
Food_ka2	−1.08 (19.9)		
Food_Tlag1	0.73 (18.2)		
WT_V_c/F	0.58 (27.9)		
WT_V_p/F	1.15 (22.5)		
Combined error model parameters			
Add. (ng/mL)	2.14 (5.82)		
Prop.	0.12 (2.27)		

WT body weight, *RSE* relative standard error, *IIV* inter-individual variability, *CV* coefficient of variation

compartment (V_c/F) and peripheral compartment (V_p/F). Parameter estimates of the final model were shown in Table 3. In the fed state, the absorption of febuxostat was expected to start later and be slower compared with the absorption in the fasted state, since the effect of food on ka and Tlag was identified negative and positive, respectively. All model parameters were estimated with a relative standard error (RSE) less than 30%. The values of eta shrinkage were relatively small in the final model (<15%).

The ability of the established model to describe the observed data can be noted by the plots showing the individual model predictions overlaid on the observations. As a representative plot shown in Fig. 3(A), the established model could capture the second peak in the fasting study and could fit the concentration-time curve of febuxostat in the fed condition. Other individual prediction plots were shown in the supplementary materials. The NPDE analysis results for the final model are presented in Fig. 3(B). The normality of the NPED was confirmed by Shapiro Wilk test. Additionally, GOF plots of the base model and final model were shown in Supplementary Fig. 1 and Supplementary Fig. 2, respectively. VPC plots stratified by dose and prandial state indicated adequate model performance were shown in Supplementary Fig. 3. Furthermore, we calculated the non-compartment $AUC_{0-\infty}$ and C_{max} of the predicted data, and compared the parameters with those of the observed data. As shown in Fig. 4, the predicted $AUC_{0-\infty}$ and C_{max} were close to the observed values.

Model simulations

Utilizing the parameter estimates from the final model, simulations in the Chinese population highlighted the effect of body weight were shown in Fig. 5. As shown in Fig. 5(B), population with a relatively higher body weight tend to have a relatively lower drug exposure, but the difference was slight in the concentration-time profiles of febuxostat.

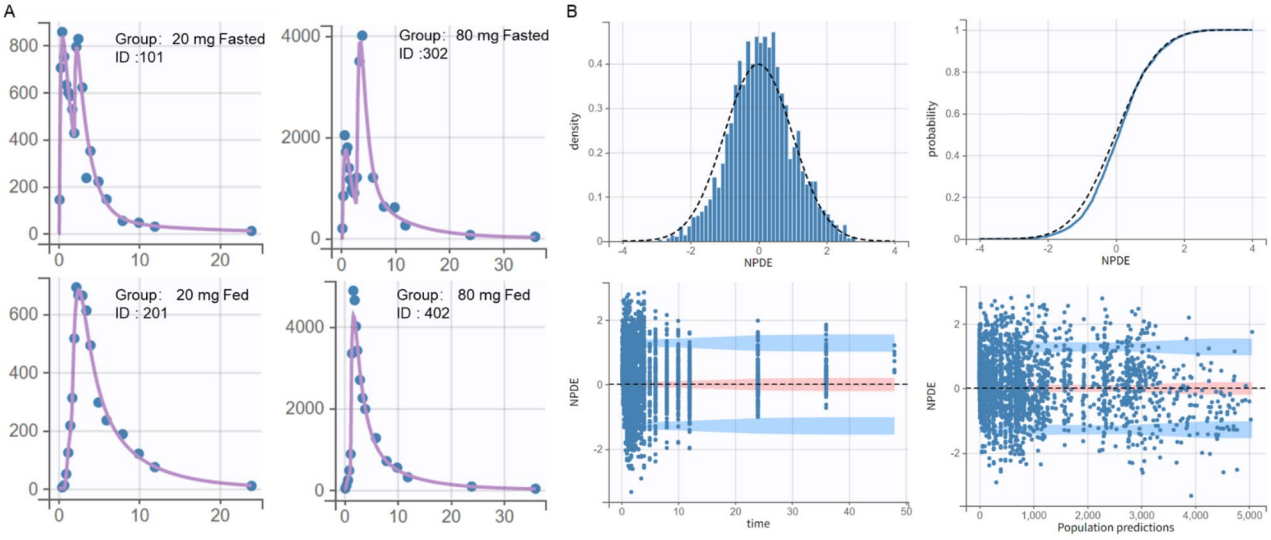

Fig. 3 Model evaluations. (**A**) Representative individual fits of the final model. (**B**) Graphs of normalized prediction distribution error (NPDE) results for the final model

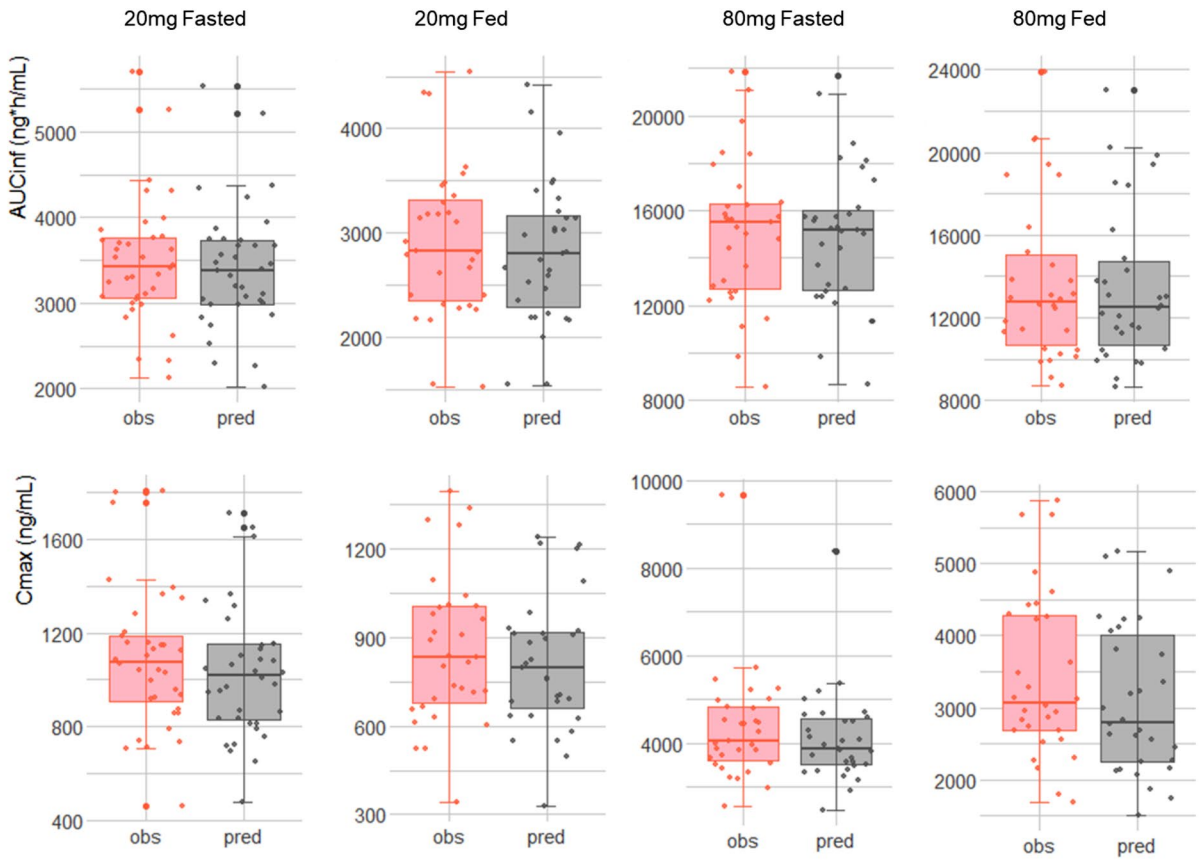

Fig. 4 Observed and predicted $AUC_{0-\infty}$ and C_{max} grouped by dose and prandial state

Based on the final model established in healthy Chinese population, simulation of concentration-time profiles in healthy Caucasian subjects was performed both under the fasted and fed condition. The bioavailability was decreased by 46%, and CL/F was increased to 6.9 L/h according to the estimates of fractional difference of race reported by Rekić et al. [13]. Other parameters remained the same. After literature search and selection, only one food effect study reported by Khosravan et al. [22] in Caucasian population was identified and included. The number of subjects of the simulated population was set to be 24, and the demographic characteristics of the subjects were in accordance with those in the reported food effect study [22]. Simulated mean concentration-time curves of febuxostat and 90% intervals in healthy Caucasian population were shown in Fig. 6. The simulated PK profiles were in consistent with the reported mean concentration-time curves for the elimination phase. And the model could predict PK profiles in the fed state in general. However, the absorption of febuxostat in the fasted state in Caucasian population was underpredicted (Fig. 6).

Discussion

In the present study, we conducted a PopPK analysis to elucidate the absorption dynamics of febuxostat in healthy Chinese volunteers and to quantify the impact of food intake on its absorption profile. Our findings revealed the multiple-peak phenomenon in the concentration-time courses of febuxostat, more prominently observed in the fasting condition than under the fed condition. Statistics in our modeling dataset showed that approximately 75.0% and 80.6% of subjects administered 20 mg and 80 mg febuxostat, respectively, in the fasting state displayed multiple peaks, and about 40% curves showed multiple peaks in the fed study. Although it should be noted that these data may be overestimated due to including of small shoulders and false count of the oscillation in terminal elimination phase by R software program, multiple-peak phenomenon of febuxostat observed in our study is surely not a coincidence. Besides, dual peaks could also be seen in other reported studies [3, 9]. A part of concentration-time profiles presented multiple peaks reflecting a short of intermittent or periodic absorption process that results in febuxostat's plasma concentration oscillation. The intermittent

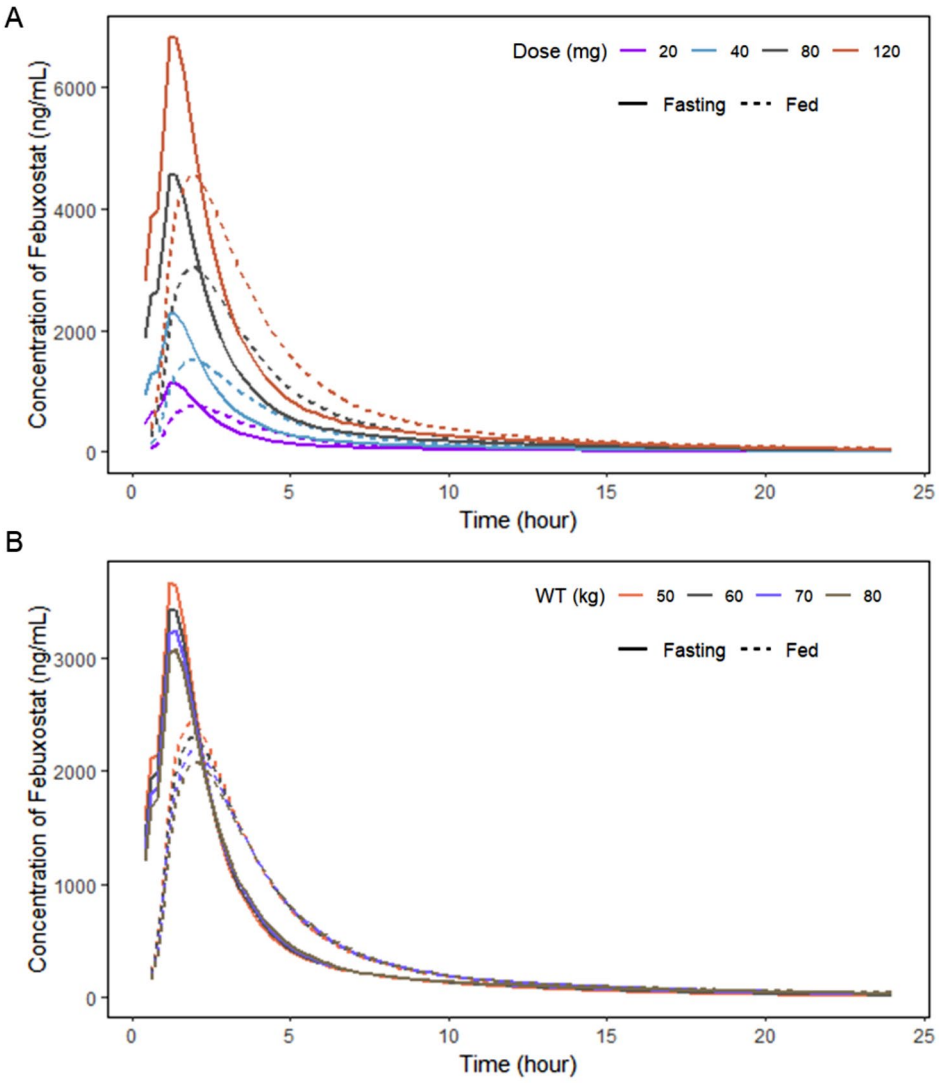

Fig. 5 Simulated concentration-time profiles of febuxostat in healthy Chinese subjects under fasting or fed condition. (**A**) Single dose of 20 mg, 40 mg, 80 mg, and 120 mg febuxostat, body weight of the simulated subject is 60 kg. (**B**) Single dose of 60 mg febuxostat, body weight of the simulated subjects are 50 kg, 60 kg 70 kg and 80 kg, respectively

or periodic absorption suggested by these profiles invites further scrutiny of febuxostat's absorption kinetics, a topic not thoroughly addressed in prior research.

Causes of secondary peaks in PK could be classified into physicochemical and formulation factors and physiological factors [23]. Physicochemical and formulation factors include solubility-limited absorption, modified-release formulation, etc., while physiological factors involve enterohepatic recirculation, gastric emptying, site-specific absorption, gastric secretion-enteral reabsorption and anesthesia and surgery [23]. Enterohepatic circulation is expected to be observed after a meal. However, the second peak is before 4 h (meal time) in this study, so the likelihood of having enterohepatic recirculation is very low. And there are no direct studies to support enterohepatic cycling of febuxostat in humans up to now. Solubility-limited absorption may be relevant to the absorption characteristics of febuxostat as it has been classified as a BCS II compound.

The abundance of early-phase data encouraged exploration of complex absorption models. We exhaustively examined various absorption models, including Weibull absorption, sequential zero- to first-order process with or without lag-time, simultaneous zero- and first-order absorption, variable absorption process, etc. Weibull absorption, simultaneous zero- and first-order absorption, and sequential zero- to first-order absorption model could not describe the multiple peaks of febuxostat. Double gamma absorption model [21] was not robust enough in our study. We found that model with variable

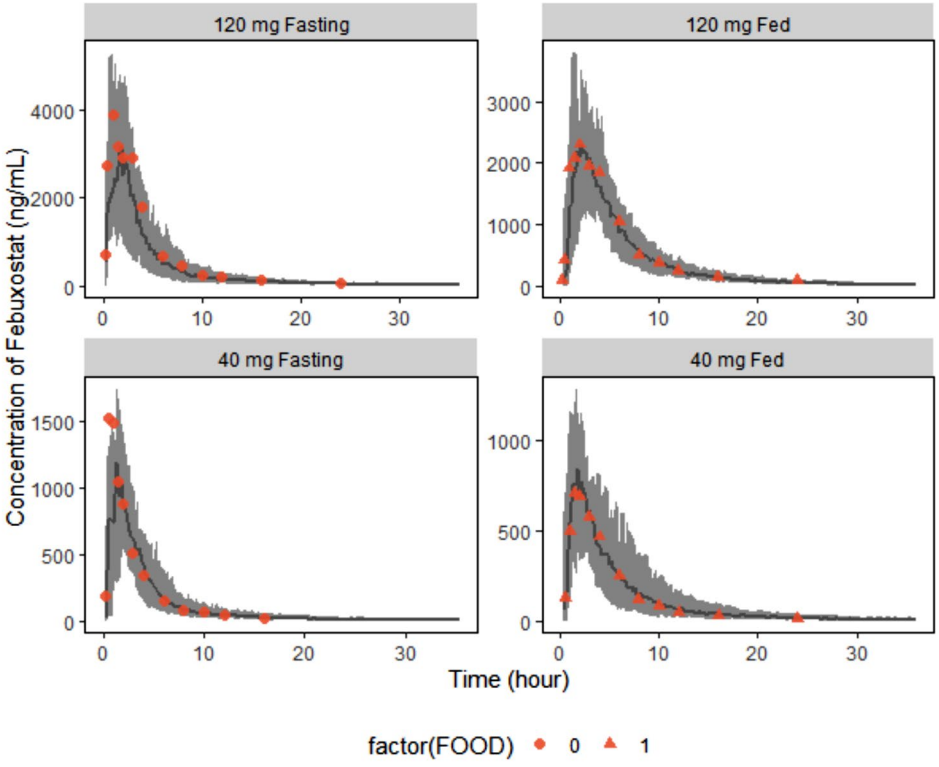

Fig. 6 Simulated concentration-time profiles of febuxostat in healthy Caucasian subjects. The red dots and triangles are the observed data, the dark grey lines are the predicted medians, the grey areas represent the 90% predicted intervals

absorption process, such as different ka after a certain time, or add a complex function on ka could simulate the multiple-peak phenomenon. The two-depot absorption model was chosen as the final model according to model stability and predictive performance. Different absorption rates over time resulting by the model may be related to different regions of the gut [24], as well as the influences of solubility-limited process, gastric emptying and food effect. Variable absorption within different regions of the gut was thought to be a probable physiological explanation for multiple-peak phenomenon and has been cited as the reason for the absorption of acebutolol [25], ranitidine [26], talinolol [27] etc.

Body weight is a common covariate identified significant for PK parameters such as distribution volume. In our study, body weight was added on V_c/F and V_p/F in the final model. The results of a PopPK analysis for febuxostat in Japanese patients showed that body weight significantly influenced CL/F and apparent volume of distribution of febuxostat [11]. It has been reported that Asian individuals have a higher febuxostat exposure than Caucasians independent of body weight [13]. We adjusted the model parameters with reference to the PopPK estimates reported by Rekić et al. [13], because it is the only reported study evaluating race difference. The estimated CL/F for healthy Chinese subjects in our study was 6.14 L/h, and the CL/F for healthy Caucasian subjects in simulation was 6.9 L/h after adjustment. This value was less than CL/F reported by Rekić et al. (14.58 L/h) [13], but was close to the estimate for healthy Australian subjects (6.91 L/h) [15]. Overall, our model adequately predicted the distribution and elimination phases in Caucasians post-adjustment.

The predicted and observed NCA parameters in healthy Caucasian population was summarized in Supplementary Table 1. The ratio of mean predicted value and observed value for C_{max}, AUC, and T_{max} in the fasted condition was 0.81, 0.92, and 1.41 respectively (average of the 40 mg and 120 mg group). In the fed state, the ratio (predicted/observed) of C_{max}, AUC, and T_{max} was 0.92, 1.13, and 1.13 respectively. The fed/fasted ratios for the observed mean parameters were 0.60, 0.83, and 1.87 for C_{max}, AUC, and T_{max}, respectively (average of the 40 mg and 120 mg group), while the predicted fed/fasted ratios for C_{max}, AUC, and T_{max} were 0.68, 1.02, and 1.53, respectively, indicting that the predicted effect of food on the PK of febuxostat was less than the observed food effect in healthy Caucasian subjects. The results of a two-compartment first-order absorption model established in healthy Australia subjects and patients showed that food reduced ka by 87% [15]. From our model results, food reduced ka1and ka2 by 87% and 66%, respectively, and

Tlag1 was increased in the fed state. Moreover, the predicted PK profiles based on the established model with adjusted parameters CL/F and bioavailability in our study were consistent with the observed PK data of febuxostat in the fed state, while the model underpredicted the C_{max} in the fasted state. This indicated that the absorption kinetics in the fasted state and the impact of food on the absorption of febuxostat may be different between Caucasian population and Chinese population.

The difference in the impact of food on the absorption of febuxostat between Caucasians and Chinese populations is likely multifactorial and may be attributed to variations in gastrointestinal (GI) physiology, and genetic heterogeneities. Factors such as variations in gut motility, stomach pH, and intestinal enzyme activity can influence drug absorption. Furthermore, variations in gut microbiota composition, which can differ between ethnicities due to dietary and genetic predispositions, can also play a role in drug metabolism and absorption [28]. Genetic polymorphisms affecting drug-metabolizing enzymes and transporters can vary between populations [29, 30], underscoring another layer of complexity. For instance, Lin et al. [10] illuminated the role of the UGT1A1 polymorphism in the Chinese population, demonstrating that individuals who were heterozygous or homozygous for the UGT1A1*6 variant experienced a notably higher AUC of febuxostat (26% increase) compared to those with the wild-type allele. Nevertheless, the genetic polymorphism in UGT1A1 alone cannot fully explain the differences between Asian and Caucasian populations, suggesting the presence of additional, as yet unidentified, intrinsic or extrinsic factors that collectively shape this intricate PK distinction.

There are some limitations in this study. Although the established final model could well characterize the observed data, the remaining IIV of K_a and Tlag were large and could not be explained by any other covariate. The largely varied concentration-time profiles (Fig. 1) among individuals may be one of the reasons. Due to the limitation of data availability, we could not establish a pooled model with different race populations and evaluate the difference of absorption and food effect among races directly. The simulation results could not lead to a robust quantitative conclusion.

Conclusion

In summary, this PopPK analysis of febuxostat in healthy Chinese volunteers, under both fasted and fed conditions, successfully characterized its PK profile and underscored the significant influence of food on absorption. Body weight was identified as a significant covariate effecting on volume of distribution. The race difference of absorption dynamics and food effect of febuxostat needs further investigation.

Supplementary Information

The online version contains supplementary material available at https://doi.org/10.1186/s40360-024-00783-1.

Supplementary Material 1

Acknowledgements

We would like to thank the participants of this study for their time and selfless contribution to the clinical trials, and we are grateful to all the staff in the Second Affiliated Hospital of Zhejiang University School of Medicine who helped conduct the clinical trials.

Author contributions

WC designed and conceived the study, analyzed the data, and wrote the original manuscript; BJ and ZR conceived the study, and supervised the work and findings of the study; DY and YH acquisited the data; HL conceived the study and revised the manuscript. All authors read and approved the final manuscript.

Funding

This work was supported by the National Major Science and Technology projects of China (No. 2020ZX09201-022).

Data availability

The data presented in this study are available on request from the corresponding author on reasonable request.

Declarations

Ethics approval and consent to participate

The bioequivalence studies were conducted according to the guidelines of the revised Declaration of Helsinki, and approved by the Human Research Ethics Committee of the Second Affiliated Hospital of Zhejiang University School of Medicine (Hangzhou, Zhejiang, China). Informed consent was obtained from all subjects involved in the study.

Competing interests

The authors declare no competing interests.

Received: 5 April 2024 / Accepted: 14 August 2024
Published online: 26 August 2024

References

1. Ernst ME, Fravel MA. Febuxostat: a selective xanthine-oxidase/xanthine-dehydrogenase inhibitor for the management of hyperuricemia in adults with gout. Clin Ther. 2009;31(11):2503–18.
2. Maddileti D, Jayabun S, Nangia A. Soluble cocrystals of the xanthine oxidase inhibitor febuxostat. Cryst Growth Des. 2013;13(7):3188–96.
3. Khosravan R, Grabowski BA, Wu JT, Joseph-Ridge N, Vernillet L. Pharmacokinetics, pharmacodynamics and safety of febuxostat, a non-purine selective inhibitor of xanthine oxidase, in a dose escalation study in healthy subjects. Clin Pharmacokinet. 2006;45(8):821–41.
4. Kamel B, Graham GG, Williams KM, Pile KD, Day RO. Clinical pharmacokinetics and pharmacodynamics of Febuxostat. Clin Pharmacokinet. 2017;56(5):459–75.
5. Grabowski BA, Khosravan R, Vernillet L, Mulford DJ. Metabolism and excretion of [14 C] febuxostat, a novel nonpurine selective inhibitor of xanthine oxidase, in healthy male subjects. J Clin Pharmacol. 2011;51(2):189–201.
6. Zhou H, Zheng Y, Wu G, Hu X, Zhai Y, Iv D, Liu J, Wu L, Shentu J. Pharmacokinetics and tolerability of febuxostat after oral administration in healthy Chinese volunteers: a randomized, open-label, singleand multiple-dose three-way crossover study. Int J Clin Pharmacol Ther. 2016;54(2):115–24.
7. Zhang M, Di X, Xu L, Xu J, Yang Y, Jiang N, Song L, Xu X. Pharmacokinetics and pharmacodynamics of febuxostat under fasting conditions in healthy individuals. Experimental Therapeutic Med. 2014;7(2):393–6.
8. Khosravan R, Kukulka MJ, Wu JT, Joseph-Ridge N, Vernillet L. The effect of age and gender on pharmacokinetics, pharmacodynamics, and safety of

febuxostat, a novel nonpurine selective inhibitor of xanthine oxidase. J Clin Pharmacol. 2008;48(9):1014–24.
9. Grabowski B, Khosravan R, Wu JT, Vernillet L, Lademacher C. Effect of hydrochlorothiazide on the pharmacokinetics and pharmacodynamics of febuxostat, a non-purine selective inhibitor of xanthine oxidase. Br J Clin Pharmacol. 2010;70(1):57–64.
10. Lin M, Liu J, Zhou H, Wu M, Lv D, Huang Y, Zheng Y, Shentu J. Wu. Effects of UDP-glucuronosyltransferase (UGT) polymorphisms on the pharmacokinetics of febuxostat in healthy Chinese volunteers. Drug Metab Pharmacokinet. 2017;32(1):77–84.
11. Hira D, Chisaki Y, Noda S, Araki H, Uzu T, Maegawa H, Yano Y, Morita SY, Terada T. Population pharmacokinetics and therapeutic efficacy of febuxostat in patients with severe renal impairment. Pharmacology. 2015;96(1–2):90–8.
12. Kamel B, Graham GG, Stocker SL, Liu Z, Williams KM, Carland JE, Pile KD, Day RO. A pharmacokinetic-pharmacodynamic study of a single dose of febuxostat in healthy subjects. Br J Clin Pharmacol. 2020;86(12):2486–96.
13. Rekić D, Johansson S, Leander J. Higher febuxostat exposure observed in Asian compared with caucasian subjects independent of bodyweight. Clin Pharmacokinet. 2021;60(3):319–28.
14. Khosravan R, Wu J, Joseph-Ridge N, Kukulka M, Vernillet L. Population pharmacokinetics and pharmacodynamics of febuxostat in a phase-II study of patients with gout. J Clin Pharmacol. Sage Publications Inc 2455 Teller Rd, Thousand Oaks. CA 91320 USA. 2005:1083.
15. Kamel B, Abuhelwa AY, Foster D, Duong JK, Graham GG, Williams KM, Pile KD, Day RO. Population pharmacokinetic modelling of febuxostat in healthy subjects and people with gout. Br J Clin Pharmacol. 2022;88(12):5359–68.
16. Soulele K, Macheras P, Karalis V. Pharmacokinetic analysis of inhaled salmeterol in asthma patients: evidence from two dry powder inhalers. Biopharm Drug Dispos. 2017;38(7):407–19.
17. Wang C, Yu Q, Jiang X, Deng Y, Sun F, Li X, Tao Y, Lin P, Ma Y, Zhu Y, Li C. Cao. A drug-drug interaction study of a novel selective urate reabsorption inhibitor, SHR4640, and xanthine oxidase inhibitor, febuxostat, in patients with primary hyperuricemia. J Clin Pharmacol. 2023;63(2):239–49.
18. Sjögren E, Abrahamsson B, Augustijns P, Becker D, Bolger MB, Brewster M, Brouwers J, Flanagan T, Harwood M, Heinen C, Holm R, Juretschke HP, Kubbinga M, Lindahl A, Lukacova V, Münster U, Neuhoff S, Nguyen MA, Peer A, Reppas C, Hodjegan AR, Tannergren C, Weitschies W, Wilson C, Zane P, Lennernäs H. Langguth. In vivo methods for drug absorption - comparative physiologies, model selection, correlations with in vitro methods (IVIVC), and applications for formulation/API/excipient characterization including food effects. Eur J Pharm Sci. 2014;57:99–151.
19. World Medical Association. Declaration of Helsinki: ethical principles for medical research involving human subjects. JAMA. 2013;310(20):2191–4.
20. Xu Y, Chen J, Yang D, Hu Y, Hu X, Jiang B, Ruan Z, Lou H. Development of LC-MS/MS determination method and backpropagation artificial neural networks pharmacokinetic model of febuxostat in healthy subjects. J Clin Pharm Ther. 2021;46(2):333–42.
21. Koloskoff K, Benito S, Chambon L, Dayan F, Marquet P, Jacqz-Aigrain E, Woillard, J-B. Limited sampling strategy and population pharmacokinetic model of mycophenolic acid in pediatric patients with systemic lupus erythematosus: application of a double gamma absorption model with SAEM algorithm. Eur J Clin Pharmacol. 2023.
22. Khosravan R, Grabowski B, Wu JT, Joseph-Ridge N, Vernillet L. Effect of food or antacid on pharmacokinetics and pharmacodynamics of febuxostat in healthy subjects. Br J Clin Pharmacol. 2008;65(3):355–63.
23. Davies NM, Takemoto JK, Brocks DR, Yáñez JA. Multiple peaking phenomena in pharmacokinetic disposition. Clin Pharmacokinet. 2010;49(6):351–77.
24. Godfrey KR, Arundel PA, Dong Z. Bryant. Modelling the double peak phenomenon in pharmacokinetics. Comput Methods Programs Biomed. 2011;104(2):62–9.
25. Mostafavi SA, Foster RT. Influence of cimetidine co-administration on the pharmacokinetics of acebutolol enantiomers and its metabolite diacetolol in a rat model: the effect of gastric pH on double-peak phenomena. Int J Pharm. 2003;255(1–2):81–6.
26. Yin OQ, Tomlinson B, Chow AH, Chow MS. A modified two-portion absorption model to describe double-peak absorption profiles of ranitidine. Clin Pharmacokinet. 2003;42(2):179–92.
27. Weitschies W, Bernsdorf A, Giessmann T, Zschiesche M, Modess C, Hartmann V, Mrazek C, Wegner D, Nagel S. Siegmund. The talinolol double-peak phenomenon is likely caused by presystemic processing after uptake from gut lumen. Pharm Res. 2005;22(5):728–35.
28. Borrello K, Lim U, Park SY, Monroe KR, Maskarinec G, Boushey CJ, Wilkens LR, Randolph TW, Le Marchand L, Hullar MA. Lampe, JW. Dietary intake mediates ethnic differences in gut microbial composition. Nutrients. 2022; 14(3).
29. Cropp CD, Yee SW, Giacomini KM. Genetic variation in drug transporters in ethnic populations. Clin Pharmacol Ther. 2008;84(3):412–6.
30. Ono C, Kikkawa H, Suzuki A, Suzuki M, Yamamoto Y, Ichikawa K, Fukae M, Ieiri I. Clinical impact of genetic variants of drug transporters in different ethnic groups within and across regions. Pharmacogenomics. 2013;14(14):1745–64.

Publisher's note